Proceedings of
ASME TURBO EXPO 2001
June 4-7, 2001, New Orleans, Louisiana, USA

2001-GT-0204

COMPUTATIONAL AND MATHEMATICAL MODELLING OF TURBINE RIM SEAL INGESTION

Nicholas J. Hills
Thermo-Fluid Mechanics
Research Centre
University of Sussex
Brighton, BN1 9QT,
UK.

John W. Chew
School of Mechanical and
Materials Engineering
University of Surrey
Guildford, Surrey, GU2 7XH,
UK.

Alan B. Turner
Thermo-Fluid Mechanics
Research Centre
University of Sussex
Brighton, BN1 9QT,
UK.

ABSTRACT

Understanding and modelling of main annulus gas ingestion through turbine rim seals is considered and advanced in this paper. Unsteady 3-dimensional computational fluid dynamics (CFD) calculations and results from a more elementary model are presented and compared with experimental data previously published by Hills et al (1997). The most complete CFD model presented includes both stator and rotor in the main annulus and the inter-disc cavity. The k-ε model of turbulence with standard wall function approximations is assumed in the model which was constructed in a commercial CFD code employing a pressure correction solution algorithm. It is shown that considerable care is needed to ensure convergence of the CFD model to a periodic solution. Compared to previous models, results from the CFD model show encouraging agreement with pressure and gas concentration measurements. The annulus gas ingestion is shown to result from a combination of the stationary and rotating circumferential pressure asymmetries in the annulus. Inertial effects associated with the circumferential velocity component of the flow have an important effect on the degree of ingestion.

The elementary model used is an extension of earlier models based on orifice theory applied locally around the rim seal circumference. The new model includes a term accounting for inertial effects. Some good qualitative and fair quantitative agreement with data is shown.

1. INTRODUCTION

In modern gas turbine engines ingestion of hot mainstream gas into the space between a rotating turbine disc and the stator can potentially lead to overheating and reduced life of the disc, and so must be controlled. To prevent or limit this effect, relatively cool air from the compressor may be channeled radially outwards through the cavity and ejected into the mainstream flow. To avoid excessive performance penalties associated with the secondary air system it is usually desirable to minimise the amount of sealing air used. This requires quantitative estimates for the relationship between sealing flow rate and hot gas ingestion. In the present contribution computational fluid dynamics (CFD) and more elementary models are considered, and calculations from these models are compared to previously published experimental data. Particular attention is focused on the complex flow interactions in the rim seal region where the sealing and mainstream flows meet.

Early work on sealing of rotor-stator disc cavities centred on the effects of disc pumping which tends to draw flow into the cavity in order to satisfy the flow requirements of the boundary layer formed on the rotating disc. For example, Bayley and Owen (1970) considered a simple axial seal in the absence of external flow and obtained a correlation for the minimum sealing flow required to prevent ingestion. With further experimental and analytical work from many workers more general methods for estimating sealing requirements under these conditions are now available. As shown by Chew (1989) and Chew et al (1991), semi-empirical methods can successfully correlate experimental data for a variety of different seal types. It may be noted that appropriate scaling parameters for this problem include a Reynolds number effect since viscosity has a direct influence on the strength of the disc pumping. These studies, in which the cavity is surrounded by a quiescent environment, are most relevant to 'inner seal' arrangements where the direct effects of the mainstream annulus flow is negligible.

The influence of external flow on cavity rim sealing, and particularly the importance of circumferential pressure variations in the annulus flow, was noted by Campbell (1978) and has been confirmed experimentally by several workers. For example, Abe et al (1979), Kobayashi et al (1984), Phadke and Owen (1988), Dadkhah et al (1991) and Hamabe and Ishida (1992) have performed experiments with various degrees of asymmetry in the annulus flow caused by guide vanes or other disturbances in the stationary reference frame. As suggested by Campbell, the presence of a circumferentially uniform external flow tends to improve sealing, while circumferential asymmetries tend to increase ingestion. Chew et al (1994) gave experimental results for ingestion with the rim seal located at various distances downstream of a row of guide vanes. The experimental measurements and order of magnitude arguments supported the conclusion that disc pumping had only a secondary effect on the degree of ingestion for conditions most representative of engine operation. In this case the Reynolds number effects are weak and a more appropriate parameter is a seal-to-annulus flow velocity ratio. The densities of the sealing and annulus flows in these experiments were very close. At engine conditions density differences are likely to be significant, so momentum or mass flux ratios may eventually prove more useful in correlating results. Some experiments including both rotor and stator blade rows have been reported by Green and Turner (1992) and Bohn et al (2000). Both sets of workers found evidence that the presence of rotor blades could improve sealing effectiveness, but Bohn et al found the opposite trend for a different seal design, and their blades had a surprisingly large effect on the pressure asymmetry due to the vanes. As will be discussed further below there is also some doubt about Green and Turner's experimental conditions. Hence the effect of rotor blades in engine conditions is still open to question.

A simple model of ingestion due to pressure asymmetries in the main flow may be constructed by assuming the length scale for circumferential variations to be much greater than the seal clearance so that the seal flow is treated as locally two-dimensional. With the cavity pressure assumed to be uniform, orifice theory is then applied at each circumferential location and the overall inflow and outflow obtained through integration. Hamabe and Ishida (1992) published such a model and proprietary methods based on this approach have been available for some time (e.g. Campbell, unpublished work). However, Chew et al (1994) concluded that this method over-predicted the level of ingestion and attributed this to the neglect of inertial effects associated with the swirl component of velocity. This conclusion drew on experimental data and the results of CFD calculations which showed the influence of the inertial terms. The 3D, steady CFD model also showed some encouraging agreement with ingestion measurements, particularly at low sealing flow rates.

Further combined experimental and CFD studies were reported by Hills et al (1997). Comparison of 3D, steady CFD solutions with pressure measurements showed good agreement at lower sealing flow rates. At higher flow rates the experimental and CFD results diverged, and this was attributed to interaction of the sealing and mainstream flows. Full details of this interaction could not be captured in the CFD model which did not include resolution of the flow through the vanes. Roy et al (2000) have also shown some agreement between steady CFD solutions and measurement from pressure tappings for a rim sealing rig including vanes and rotating blades. In another very recent paper Bohn et al (2000) included 3D, unsteady CFD calculations including both vanes and blades. They showed some differences in the calculated and measured levels of ingestion but obtained some qualitative agreement. It may be noted that most research has concentrated on the seal downstream of a row of stationary vanes. Arguably, more work is needed to clarify the flow mechanisms in seals downstream of a row of rotating blades.

In recent years there has been increasing interest in the influence of sealing flows on the aerodynamic efficiency of the main annulus flow. Denton (1993) noted this effect, and likens the flow mixing process to that of leakage flow over a shroud. A first estimate of the mixing losses might be obtained from the formulae given by Denton or Hartsel (1972). Denton notes that most of the entropy generation will be due to the difference in swirl velocity between the two flows and recommends pre-swirling the sealing flow where possible. Recent studies of turbine shroud leakage flows by Wallis et al (2000) and Pfau et al (2000) showed the importance of non-axisymmetric effects on the flow through the axial gaps upstream and downstream of the shroud. The flow fields identified are similar to those associated with the ingestion problem. Recent studies of stator shroud leakage in compressors are also of interest to the present study. For example, Wellborn and Okiishi (1998) report both experimental and CFD results. These indicate that the effect of leakage flow on the blading aerodynamics can result in higher losses than would be expected from simple mixing. Demargne and Longley (2000) conclude from experiments and computations for a linear cascade that pitchwise non-uniformities in the flow can lead to exchange of fluid across the axial gap upstream of a row of vanes, and that this contributed to loss generation.

CFD solutions for mainstream gas ingestion across a simple axial rim seal are presented in section 3 below. These results are also compared to measurements from the experimental rig previously presented by Hills et al (1997). For completeness a brief description of the rig is given in section 2. Further discussion of the results and the flow physics are given in section 4 which includes comparison with a more elementary model. The main conclusions from this study are summarised in section 5.

NOMENCLATURE

C_d	discharge coefficient
C_h	loss coefficient
l	length scale for seal flow
m	inlet mass flow to disc cavity

m_{in}	ingestion mass flow rate
m^*	non-dimensional ingress flow rate = $m_{in}/2\pi\rho s_c r_o u_{ax}$
n	number of blades or vanes
p	static pressure
p_c	static pressure in disc cavity
r	radial coordinate
r_o	inner annulus wall radius
s_c	seal clearance
u	radial component of velocity
U	representative velocity for the seal flow
u_{ax}	axial component of mean annulus velocity
u_m	mean velocity through seal = $m/2\pi\rho s_c r_o$
$\underline{u}_s$	= (u,0,w)
u_s	magnitude of $\underline{u}_s$
v	tangential component of velocity
w	axial component of velocity
z	axial coordinate
Δp	pressure difference across seal
Δp^*	= $\Delta p/\rho u_{ax}^2$
μ	viscosity
θ	angular coordinate in cylindrical system
ρ	density
Ω	angular velocity of rotor
Φ	sealing effectiveness or species concentration

Subscripts

1	refers to stationary vanes
2	refers to rotating blades or pegs

2. EXPERIMENTAL RIG

The experimental rig has been fully described by Green (1994). A schematic diagram of the rig is given in fig. 1. The rig consists of a rotor-stator system enclosed by an annular channel in which 29 nozzle guide vanes are positioned with the trailing edge 3mm upstream of the rim seal gap. Mainstream flow is drawn through the annulus by a centrifugal fan, located well downstream of the cavity under investigation, and hence total pressure and temperature upstream of the vanes are atmospheric. The plain rotor was driven by 16 aluminium pegs attached to the periphery of the discs and located 18.5mm downstream of the seal gap. The 16 equispaced pegs were manufactured from cylinders of 19mm diameter and height 24mm with a flat surface milled on them as shown in fig. 2.

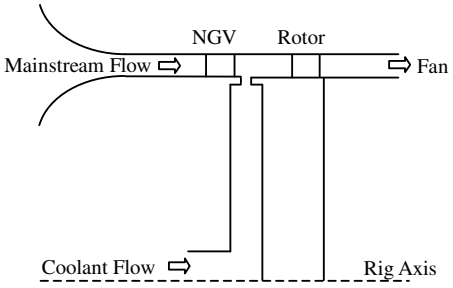

Fig. 1. Schematic of Experimental Rig.

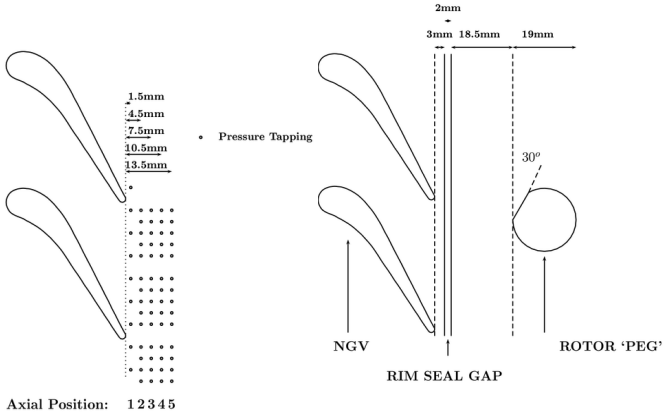

(a) Pressure tappings in unbroken annulus

(b) Positions of vanes and rotor 'pegs'

Fig. 2. Schematic showing guide vanes, pressure tappings and rotor pegs.

Some experiments were carried out with the rim seal gap blocked off, providing an unbroken annulus. In these cases static pressure measurements were made at 5 axial locations downstream of the vanes, as shown in fig. 2. With the seal gap present annulus static pressure measurements were possible only at the first axial location. Pressure tappings in the cavity were located on the stator face at nine radial locations with the outermost location being at r/r_o=0.95. Mainstream flow ingestion was quantified through concentration measurements with the coolant seeded with about 450ppm of nitrous oxide. Sampling of the air in the cavity was made at 4 radial positions on the stator.

For the measurements presented in this paper, the seal gap was 0.002m, the radial extent of the seal gap was 0.003m, the outer radius of the cavity was 0.2m, the cavity width was 0.015m, and the outer radius of the annulus was 0.23m.

3. CFD SOLUTIONS

3.1 Description of the CFD Models

A commercially available CFD code (FLUENT5, 1998) was used in these studies. This code allows use of unstructured meshes in solving the Reynolds-averaged compressible Navier-Stokes equations and has been preferred to the proprietary code used by Hills et al (1997) because of its capability for modelling complex geometries. The numerical solutions were obtained using a pressure correction algorithm, and with the k-ε model of turbulence using standard wall functions at the near-wall mesh points. To quantify ingestion of mainstream gas into the disc cavity, a species concentration equation was solved. Thus, although a different code is used from earlier studies the numerical treatment and modelling assumptions are similar to those employed in earlier validation work on the disc cavity and rim sealing flows (see, for example, Virr et al, 1993). Although

they are not reported here, several benchmark tests for disc cavity flows have been repeated using FLUENT. It may be noted, however, that the validation does not include examples of turbomachinery blading flows. This point, and some preliminary investigations into the use of alternative turbulence models, will be discussed further below.

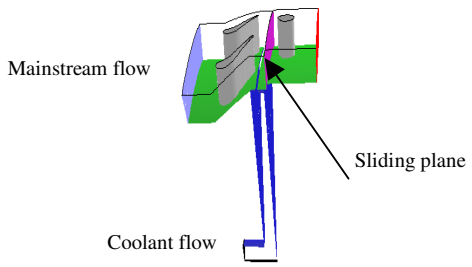

Fig. 3. Computational Domain for Model 4.

Four different CFD models are used and these are summarised in table 1. All models included the disc cavity and the same section of the annulus, but differ in treatment of the vanes and rotor pegs. All the models assumed 29 guide vanes (as were used in the experiment) and where rotor 'pegs' were modelled, 1 rotor peg per 2 guide vanes was used. This corresponds to 14.5 rotor 'pegs' as compared to 16 in the experiment. The most complete representation is given by model 4, for which the computational domain is illustrated in fig. 3. This model calculates the unsteady flow with the solution for rotating and stationary parts of the domains being communicated across a sliding plane. Model 1 does not include the rotor pegs and assumes steady flow in the stationary frame (and models only one NGV passage compared to figure 3). Model 2 does not include the vanes and assumes steady flow in the rotating frame. Model 3 includes both vanes and pegs, but with a mixing plane (placed between the vane trailing edge and the rim seal gap) across which circumferentially averaged solutions are exchanged between the main steady (in the rotating reference frame) calculation for the rotor pegs and cavity and an auxiliary steady (in the stationary reference frame) calculation for the vanes. For the CFD calculations presented here, the conditions corresponded to a rotational Reynolds number ($\rho\Omega r_0^2/\mu$) of 10^6, a mainstream Reynolds number ($\rho u_{ax} r_0/\mu$) of $5.9\text{x}10^5$, and a coolant flow rate such that the velocity ratio u_m/u_{ax} (the continuity-derived mean velocity through the seal divided by the axial component of the annulus velocity) was $4.8\text{x}10^{-2}$.

Periodicity in the circumferential direction was assumed at the appropriate boundaries, and the usual no-slip conditions were applied on solid surfaces. At the sealing flow inlet, the normal velocity component was set to a uniform value so as to give the required mass flow, other velocity components were set to zero, and the species concentration was set to unity. In the annulus, total pressure, total temperature, flow angle and a species concentration of zero were specified at the inlet. For models including the vanes these inlet conditions were essentially atmospheric with allowance for boundary layers on the annulus walls. The boundary layer profile for a constant section annulus of the same length as the section of the rig upstream of the guide vanes was used. For model 2, the annulus inlet conditions were assumed to be uniform. Effectively the difference between models 2 and 3 is that model 3 uses the radial profiles from the vane exit instead of a uniform profile. At the flow exit, static pressure was specified at the hub, the pressure distribution was obtained from the radial equilibrium conditions, and zero axial gradient was assumed for other variables. While the unsteady solution did not include any special treatment to avoid reflections of waves at the boundaries, the boundaries were placed some distance from the blades and the solutions were found to show little unsteadiness at the inlet and exit.

Table 1. Summary of CFD models.

Model No.	Steady / Unsteady	No. vanes	No. rotor pegs
1	Steady in stationary frame	1	0
2	Steady in rotating frame	0	1
3	Steady (with mixing plane)	2	1
4	Unsteady (with sliding plane)	2	1

Mesh generation was performed using the FLUENT mesh generator and unstructured quadrilateral meshes were used for all models. $5\text{x}10^5$ mesh points were used for model 1; $7\text{x}10^5$ mesh points were used for model 2; and 10^6 mesh points were used for models 3 and 4. In all the models, boundary layer meshes (using 5 layers of prisms) were grown away from the solid surfaces at a geometric growth rate of 1.2, and 30 mesh points were used to span the cavity in an axial direction to ensure that the cavity velocity gradients were resolved. The unsteady solution was obtained using implicit time stepping with a time step of $2\text{x}10^{-5}$s (so approximately 30 time steps were used per pass of a rotor blade by a guide vane). Under-relaxation was used in the pressure correction algorithm for the solution of the steady flow solutions and for calculating the solution at each time step in the unsteady solution.

3.2 Convergence of Solutions

Convergence of the iterative steady state solutions was monitored using the residuals of the continuity, momentum, concentration and turbulence model equations. Typically 4-5 orders of magnitude reduction was achieved after about 5000 iterations. These calculations took about 12 hours CPU time on a cluster of 8 666MHz PCs.

Convergence of the unsteady solution was given careful consideration. Whereas in 'blading flow only' calculations it is quite usual for convergence to periodicity to occur after about 10 blade passing cycles, the solution in the disc cavity for the present model took considerably longer to converge. This may

be attributed to the lower velocities within the disc cavity. Radial velocities in the cavity are typically 5 m/s or less. Thus an element of fluid will take about 0.01 s (or about 200 blade passing cycles) to traverse the cavity. Convergence of the solution physically requires at a minimum for the ingested mainstream particles to re-circulate the cavity, and hence the solution will require several times this amount of physical time to converge.

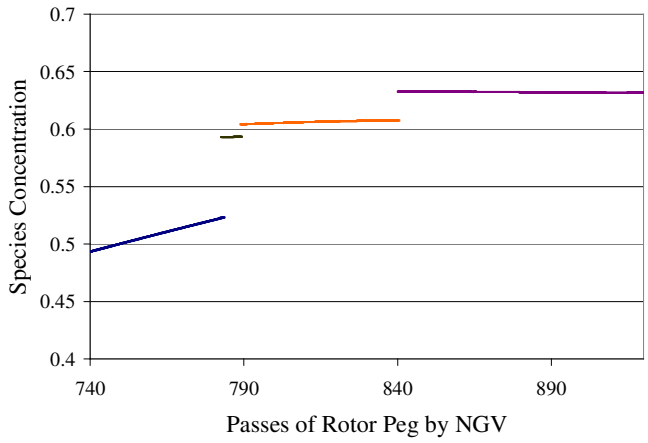

Fig. 4. Convergence of concentration at r/r_0=0.41 stator measurement point for unsteady solution.

The convergence of the concentration in the cavity (at the measurement point r/r_0=0.41 on the stator) is shown in figure 4. As can be seen, after the unsteady simulation had proceeded for 780 periods the species concentration in the cavity was still observed to be changing significantly, although this is only obvious over a considerable number of periods. At this point the unsteady solution was suspended. A steady state species concentration equation was then solved for the region of the cavity with $r \leq 0.15$ m using fixed velocity and turbulence fields from the last time point of the unsteady solution. The boundary conditions specified at r = 0.15 m were also taken from the unsteady solution. Since the flow in this inner region had been observed to be essentially steady, the steady concentration equation would be expected to show little change from a converged unsteady solution. However, the steady solution showed significant changes from the unsteady solution, which can be seen as the discontinuities in figure 4. Restarting the unsteady solution using the revised concentration in the region $r < 0.15$ m produced further changes in the solution. Several repeats of this procedure gave a solution where the concentration remained approximately constant for some 80 periods. While it is accepted that this solution is not absolutely converged, it is believed that any further changes would be small in relation to the differences between the various models and the experimental data discussed below.

With the unsteady solution taking about 8 CPU minutes per time step (or 4 hours per period) on 8 PCs, the calculation was halted after a total simulation time of about 920 periods. At this point the solution appears to be close to convergence to periodic behaviour. With dedicated use of 8 processors of the PC cluster used it is estimated that this calculation would take about 3 months if run continuously.

3.3 Comparison with Pressure Measurements

Pressures were measured using tappings in the inner annulus wall just downstream of the vanes, and on the stator in the disc cavity, as described in section 2. Thus these measurements will not capture the unsteady variations at blade passing frequency. Comparisons of CFD results with these measurements are shown in figures 5 to 7. The mainstream pressures are plotted as an annular pressure coefficient, C_{pa}, defined as the difference between the mainstream pressure and the average mainstream pressure, non-dimensionalised by the mainstream inlet dynamic head. The static pressure asymmetry coefficient in figure 6 is defined as the maximum annulus static pressure coefficient minus the minimum annulus static pressure coefficient. The cavity pressures in figure 7 are plotted as a cavity pressure coefficient, C_{pc}, defined as the difference between the cavity pressure and the cavity pressure at r/r_0=1, again non-dimensionalised by the mainstream inlet dynamic head. In all the figures, where circumferential location is given as a fraction of NGV pitch, 0 represents a trailing edge position.

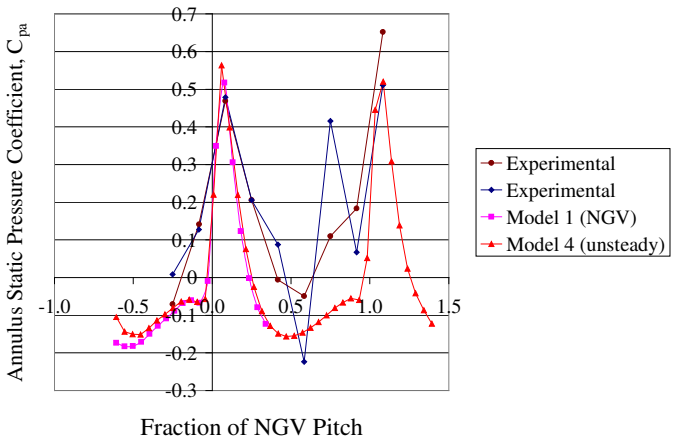

Fig. 5. Comparison of calculated and measured annulus pressures.

The annulus pressures are given in figure 5. For the unsteady solution the values plotted for the annulus represent time averages over a period. There is little difference between model 1 (modelling the vane only) and the time average of model 4. However, for the circumferential variation of pressure, agreement with the experimental data is only fair. Looking at the experimental data, it is clear that there is considerable scatter. Two sets of experimental data (measured at different

circumferential locations) are plotted, and there are significant differences between these. Neither set repeats exactly over the guide vane period. Since the unsteady pressure variation due to the rotor blades is approximately +/- 15% of the inlet mainstream dynamic head, it is possible that this variation in the experimental data is due to the unsteady effects.

Figure 6 shows the axial decay of the circumferential pressure asymmetries from CFD calculations (for both the guide vane alone and rotor 'peg' alone) for an unbroken annulus. The experimental data for the guide vane alone with an unbroken annulus are included. Also included on this figure are the decay rates from a simple potential flow model discussed by Hills et al. (1997). The difference in decay rate between the vane alone and the rotor alone in the potential flow solution is simply due to the spacing between the blades, indicating that the number of blades and hence the rate at which the resulting pressure asymmetry will decay is important for their effect on ingestion. Agreement between CFD and measurement for the asymmetry due to the vanes is fair, with the CFD apparently under-predicting the pressure variation. Earlier CFD calculations for this case by Hills et al. (1997) showed slightly better agreement with the data. This is possibly because the earlier calculations were done using a CFD code that had been specifically developed and validated for turbo-machinery applications.

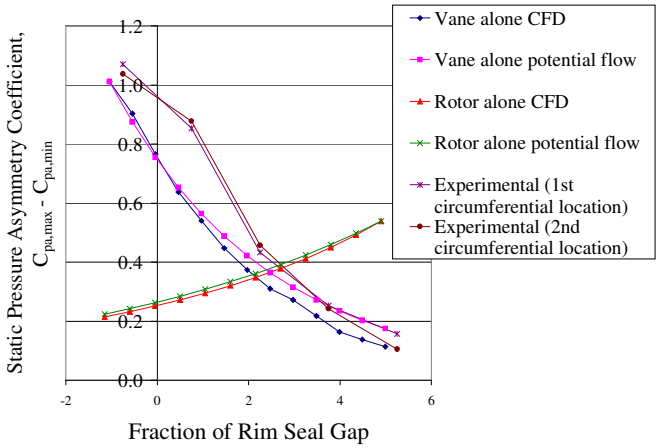

Fig. 6. Static pressure asymmetry due to vane alone and rotor 'peg' alone.

Figure 7 shows the stator disc cavity pressures. The unsteady CFD solution at the cavity measurement positions showed negligible variation with time. All the models under-predict the pressure rise in the cavity, with the unsteady model being closest to the measured value. This is possibly because (as discussed in section 3.4 below), all the models under-predict mainstream ingestion to some extent. The ingestion of highly swirled mainstream flow increases the core rotation rate in the cavity and leads to a higher pressure rise. Comparing with the concentration measurements shown in figure 8 and discussed below, the models show increasing pressure rise with increasing levels of ingestion. A further factor is the modelling assumptions for the cavity flow at inlet.

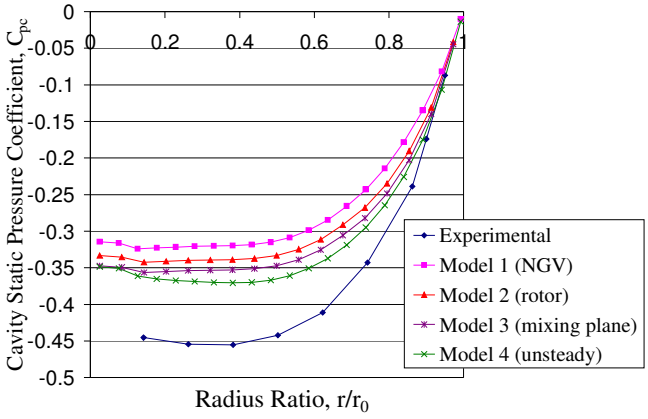

Fig. 7. Comparison of calculated and measured disc cavity pressures.

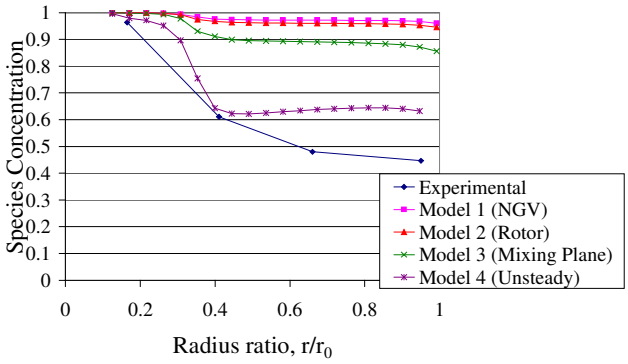

Fig. 8. Comparison of calculated and measured concentration in the cavity.

3.4 Comparison with Concentration Measurements

Fig. 8 shows the measured and calculated species concentration in the disc cavity at the stator tapping positions. In contrast to the cavity pressures, there are very significant differences between the various CFD models. Note that according to the unsteady calculation the concentration at these positions is essentially constant.

All the models under-predict the level of ingestion, but agreement between the unsteady CFD model and the measurements is closest, and this calculation is considered very encouraging. Note that the under-prediction of the annulus pressure asymmetry (as noted above) may contribute to the under-prediction of ingestion. It is clear from comparison of the CFD solutions that, for these conditions, the combined effect of

the rotor asymmetries gives considerably more mainstream gas ingestion than either the rotor or stator acting alone. As could be seen from figure 6, the circumferential pressure asymmetry at the seal due to the vane alone was approximately twice that from the rotor alone. However, despite this, the rotor asymmetry can apparently cause greater ingestion than the stator asymmetry, depending on the inlet profile used. This is attributed to the near coincidence of annulus flow tangential velocity and rotor speed when the mixing plane model was used. The importance of tangential velocity will be discussed further in section 4 below.

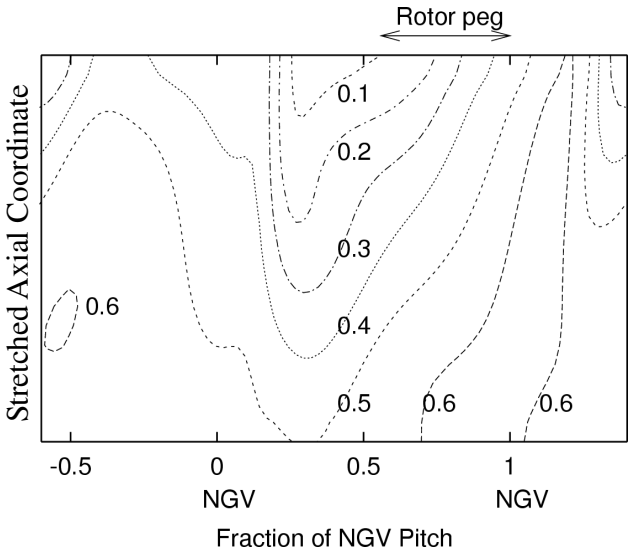

(a) Time Point A

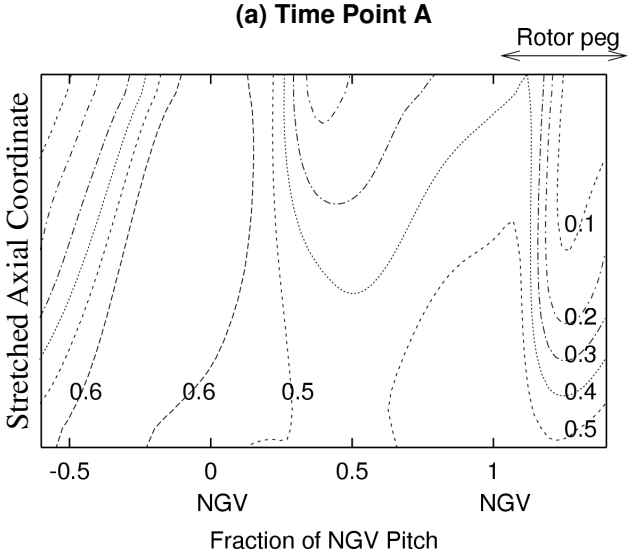

(b) Time Point B

Fig. 9. Contours of instantaneous concentration on the radial plane in the seal gap 1mm inboard of the inner annulus wall for two rotor 'peg' positions.

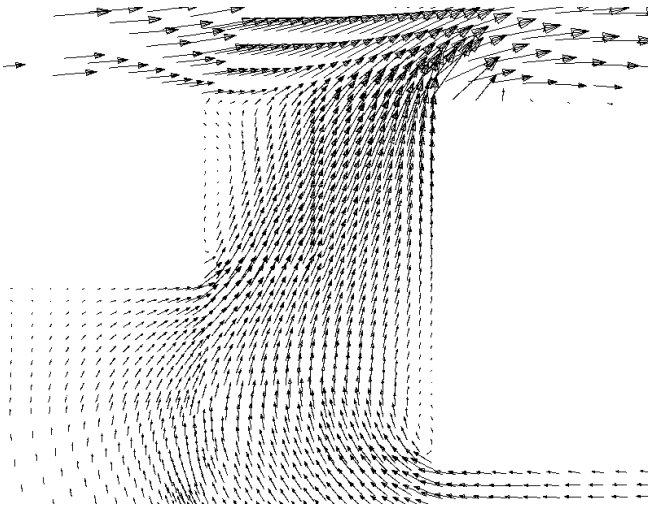

(a) Fraction of NGV pitch = 0

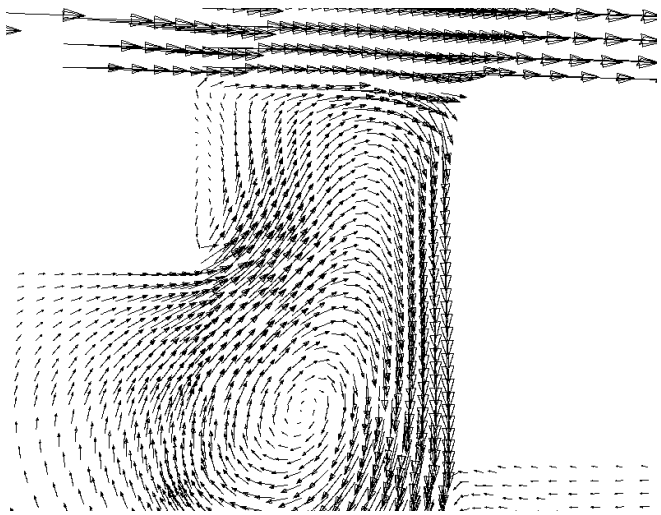

(b) Fraction of NGV pitch = 0.5

Fig. 10. Instantaneous velocity vector plots (axial-radial plane) at time position A.

3.5 Further Discussion of Results

Contours of concentration in the rim seal gap (in a radial plane 1mm inboard of the inner annulus wall) at two time instants from the unsteady solution are shown in figure 9. (The rim seal gap has been scaled to enable the detail to be seen. The bottom of the figure corresponds to the stator and the top to the rotor.) It can be seen that the ingestion occurs primarily in two regions close to the rotor driven by the pressure maxima from the two guide vanes. The difference in ingestion levels in these two regions is due to the position of the rotor 'peg'.

As has been shown in earlier studies, the flow in the rim seal region is quite complex. This is illustrated by the vector

plots in the axial-radial plane in figure 10. These are from the unsteady solution at time point A. The vector plots are given for two circumferential positions: the trailing edge of one NGV (corresponding to the NGV pitch fraction of 0 in figure 9) and midway between the NGVs (corresponding to the NGV pitch fraction of 0.5). As can be seen from these plots (and also from figure 9), ingestion is mainly occurring midway between the NGVs, while the coolant flow is exiting at the NGV trailing edge position.

The static pressure, radial velocity, and concentration along a line 0.1 mm from the rotor in the plane of figure 9 are shown in figure 11. (The static pressure is again non-dimensionalised as the difference between the static pressure and the circumferentially averaged static pressure, divided by the mainstream inlet dynamic head. The radial velocity is non-dimensionalised by the rotor disc velocity.) The time-averaged values and the vane alone values are very similar. Also plotted are the values from the unsteady solution at two time instants to show the level of variation with time. The increase in concentration in the cavity in the unsteady solution would appear to be due to the increase in mixing between the rim seal flow and the cavity recirculation due to the high frequency variation in radial velocity imposed by the rotor pegs. The level of unsteadiness in both concentration and radial velocity is clearly significant. Splitting the u and Φ into average and fluctuating components (**u**,**Φ** and u', Φ') the radial flux of the species will depend on the product **uΦ** and the time mean of the fluctuating components u'Φ'. Thus a loose analogy may be drawn between the extra ingress due to the unsteadiness and turbulent mixing.

A further point that may be noted from figure 11 is the circumferential displacement of the positions of maximum and minimum radial velocity from the positions of minimum and maximum static pressure. This is due to the swirl component of the flow and confirms that inertial effects are significant.

The deterioration in sealing effectiveness in the CFD solutions due to the rotor 'blades' is in contrast to Green and Turner's (1992) conclusions. Reappraising Green and Turner's experimental results in the light of the present study it seems most likely that the presence of rotor blades in their experiment did contribute to ingestion measured, but that their estimate of the level of ingestion due to the guide vanes alone was in error. There is some uncertainty about the source of the 'vanes-only' measurements reported by Green and Turner.

As noted in section 3.1 the CFD model used was not validated for blading flow calculations. Examination of the steady solution for the vanes showed an unexpected loss of total pressure in the core of the flow. This solution was repeated (in FLUENT) using the Spalart-Allmaras turbulence model which is favoured by some workers for blading aerodynamic calculations. The Spalart-Allmaras model showed significantly lower total pressure loss although the predicted pressure asymmetry was similar to that given by the k-ε model in figures 5 and 6. (Although the Spalart-Allmaras model predicted approximately 5% greater pressure asymmetry.) However, further testing of the Spalart-Allmaras model indicated some problems with this model in predicting flows in rotating disc cavities. Thus, at present, the choice of turbulence model depends on whether the primary interest is in the disc cavity or blading flows. Further work is planned to arrive at a turbulence model which will give a good representation of both the blading and disc cavity flows.

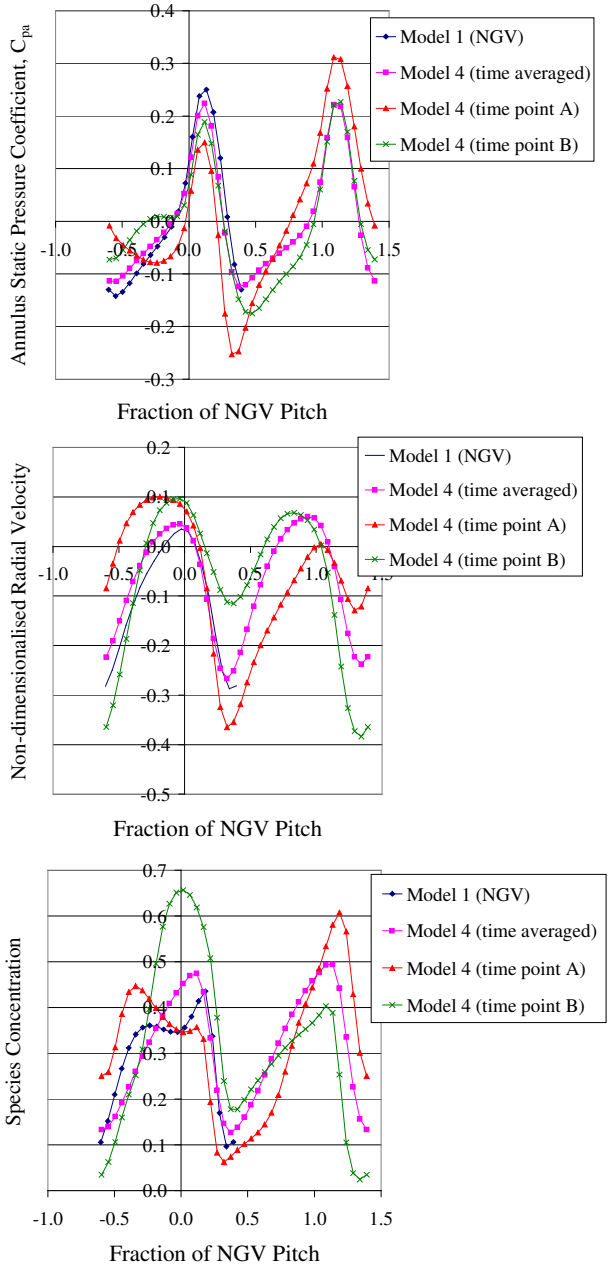

Fig. 11. Pressure, radial velocity and concentration in the rim seal gap on the line 0.1mm from the rotor, and 1mm radially inboard of the inner annulus wall.

4. THE SIMPLE MODEL

4.1 Description of the Model

Assuming inviscid flow the equations expressing conservation of momentum in the radial and axial directions may be written.

$$\frac{\partial u}{\partial t}+u\frac{\partial u}{\partial r}+\frac{v}{r}\frac{\partial u}{\partial \theta}+w\frac{\partial u}{\partial z}-\frac{v^2}{r}=-\frac{1}{\rho}\frac{\partial p}{\partial r} \qquad (1)$$

$$\frac{\partial w}{\partial t}+u\frac{\partial w}{\partial r}+\frac{v}{r}\frac{\partial w}{\partial \theta}+w\frac{\partial w}{\partial z}=-\frac{1}{\rho}\frac{\partial p}{\partial z} \qquad (2)$$

where (u,v,w) is the velocity in a cylindrical coordinate system (r,θ,z), t is time, ρ is density, and p is static pressure. Multiplying eqns (1) and (2) by u and w respectively, summing the two equations, and performing some algebraic manipulation gives:

$$\frac{u}{\rho}\frac{\partial p}{\partial r}+\frac{w}{\rho}\frac{\partial p}{\partial z}+\frac{\partial (u_s^2/2)}{\partial t}+u\frac{\partial (u_s^2/2)}{\partial r}+ w\frac{\partial (u_s^2/2)}{\partial z}+\frac{v}{r}\frac{\partial (u_s^2/2)}{\partial \theta}-\frac{uv^2}{r}=0 \qquad (3)$$

where

$$u_s^2=u^2+w^2 \qquad (4)$$

For the flow across the seal it is reasonable to assume low Mach number or incompressible conditions. Eqn (3) may then be expressed in vector notation as follows.

$$\underline{u}_s.\underline{\nabla}\left(p/\rho+u_s^2/2\right)+u_s\left(\frac{\partial}{\partial t}+\frac{v}{r}\frac{\partial}{\partial \theta}\right)u_s-\frac{uv^2}{r}=0 \qquad (5)$$

where

$$\underline{u}_s=(u,0,w) \qquad (6)$$

It may be noted that for steady flow with v=0, eqn (5) reduces to Bernoulli's theorem, giving conservation of total pressure along streamlines.

Some further approximation is needed to arrive at the simplified model for the seal. Changes in tangential velocity through the seal are assumed small relative to changes in the other velocity components. A characteristic value of $\underline{u}_s$ is then chosen as the velocity in the vena contracta, denoted U, and integrating in the r-z plane across the seal, the following result is deduced from eqn (5).

$$\rho l\left(\frac{\partial}{\partial t}+\frac{v}{r_o}\frac{\partial}{\partial \theta}\right)U+\frac{\rho U^2}{2}C_h\,\mathrm{sgn}(U)=\Delta p \qquad (7)$$

where C_h is a loss coefficient, *l* is an appropriate length scale (in the r-z plane), r_o is the inner annulus wall radius which is taken to equal the seal radius, and Δp is the pressure in the cavity minus the annulus pressure. This equation was proposed by Cargill (1991) who gives an alternative derivation based on Crocco's equation.

Eqn (7) is relatively straightforward to represent in finite difference form and solve numerically. This was done using central differencing for derivatives with respect to θ, and backward differencing in time. Mass flows into and out of the cavity were calculated from the computed solutions for U, which required specification of seal clearance (s_c) and discharge coefficient (C_d). An estimate of the sealing effectiveness is then given by

$$\Phi=m/\left(m+m_{in}\right) \qquad (8)$$

where m is the net mass flow rate through the seal and m_{in} is the ingestion flow rate. This estimate is based on a fully mixed assumption for the flow in the cavity. It does not fully account for the unsteady effects shown in the CFD solution and discussed above. Derivation of the above equation involves the assumption that the concentration of outflow through the seal is at the mixed value for the cavity and inflow is at the annulus inlet concentration. Looking at figures 8and 10 from the CFD solution suggests that this may be a reasonable approximation.

For the calculations described below C_h was taken as 1 and discharge coefficients were obtained from the correlations given by Chew et al (1994). These give the discharge coefficient as a function of the ratio of mean seal velocity to the axial component of the annulus velocity (u_m/u_{ax}). Accuracy of the numerical solutions was tested by comparison with analytical integration of a sine function, by varying mesh spacing and time step, and by verifying that with appropriate coordinate transformation a transient solution with v=0 was equivalent to a steady solution with the appropriate value of v.

A shortcoming of the above model is the need to specify *l* and v. Here *l* was set to $C_d.s_c$ and v was set to the estimated swirl velocity for the annulus flow above the seal. Note that effects arising from differences in tangential velocity between the cavity and annulus flows are not modelled. Sinusoidal variations of annulus static pressure are assumed with uniform and steady cavity pressure. The cavity pressure is varied to obtain results for a range of sealing mass flows.

4.2 Comparison with Measurements

Fig. 12 shows a comparison of results from the simple model with the data given by Chew et al (1994). In this case the pressure asymmetry in the annulus is caused by a row of 18

guide vanes at different axial positions (NGV=1 or 3) upstream of the seal. Predictions from the model are given with pressure asymmetries equal to 0.5 and 1.5 times the axial dynamic head for the annulus. These conditions are representative of the extremes of the experimental range. Calculations are also given for v=0 and v= 96 m/s which is an estimate of the experimental annulus swirl velocity. For v=0 (and no time dependency of Δp) the inertial term in eqn (7) vanishes, and the model reverts to the straightforward orifice flow approximation used by other workers. As shown by Chew et al, without the inertial terms the model over-predicts the degree of mainstream ingestion. Inclusion of the inertial term gives much better quantitative agreement with the data at low sealing flow rates, although the model shows greater sensitivity to the level of pressure asymmetry than measured experimentally. At higher sealing flow rates the experimental and calculated results show different trends, possibly due to complex interaction of the sealing and annulus flows.

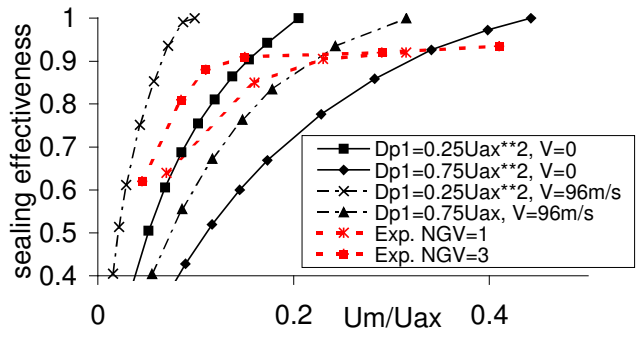

Fig. 12. Comparison of simple model with data from Chew, Green, and Turner (1994).

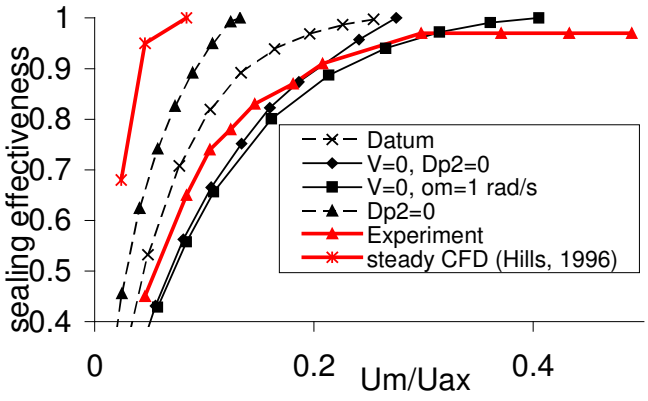

Fig. 13. Comparison of simple model with data from the present configuration.

Comparisons of model predictions of sealing effectiveness with data from the rig described in section 2 are shown in fig. 13. In these calculations Δp has been specified as follows.

$$\Delta p = p_c - \left[1+\sin\left(n_1\theta\right)\right]\frac{\Delta p_1}{2} - \left[1+\sin\left(n_2\left(\theta-\Omega t\right)\right)\right]\frac{\Delta p_2}{2} \quad (9)$$

where n is the number of blades or vanes, and subscripts 1and 2 refer to the stator and rotor, respectively. Estimating experimental conditions, the following values are assumed.

v=87 m/s, Ω=428 rad/s, n_1=29, n_2=16, Δp_1 =1000 Pa, Δp_2 =600 Pa (10)

where Ω is the angular velocity of the rotor, and Δp_2 has been estimated entirely from the CFD solution, no unsteady or rotating measurements being available. Values of some of these parameters were varied to show sensitivity of the model.

Looking first at the comparison between results for the base conditions given above and the measurements shows some fair agreement at low sealing flows, but differences at higher flow rates. Again sealing/annulus flow interaction may account for some of this effect. Neglecting the pressure asymmetry due to the rotor and the inertial terms (Δp_2 = v =0) leads to over-prediction of ingestion at low flow rates. For v=0, Ω=1 rad/s the inertial terms in eqn (7) will be negligible but the computed solution will include a quasi-steady representation of the rotor pressure asymmetry. The calculated sealing effectiveness is close to that of the Δp_2 = v =0 solution at low flows, but a higher flow rate is required to fully seal the cavity. Without the inertial terms, the model requires Δp≥0 in order to prevent ingestion. Thus for the quasi-steady solution a higher cavity pressure (and hence higher flow rate) is required for complete sealing.

The effect of the pressure asymmetry due to the rotor, as predicted by the model, is shown by comparing calculations for the base condition with those for Δp_2 =0 in fig. 13. As for the CFD solution in section 3, without the rotor pressure asymmetry ingestion is significantly reduced. This fig. also includes steady CFD results from Hills' (1996). This CFD was based on the model presented by Hills et al (1997) and models the annulus flow asymmetry due to the vanes using a potential flow approximation. The under-prediction of ingestion due to this model (despite some good agreement with pressure measurements) is in qualitative agreement with the simple model.

As mentioned in the introduction, and in section 3, Green and Turner (1992) concluded from their experimental studies that the presence of rotor blades may help reduce ingestion. Although based on a different configuration to that considered here, this seems to conflict with present results. Further studies with the simple model confirm that is does not predict any

improvement in sealing due to rotating blades. The balance of evidence indicates that the presence of blades will usually tend to increase ingestion. Note, however, that the flow through the seal is complex with elements of fluid oscillating radially as they pass through regions of positive and negative pressure gradient. Thus considerable uncertainty remains about the validity of the simple model. More measurements and CFD studies are needed to clarify this issue.

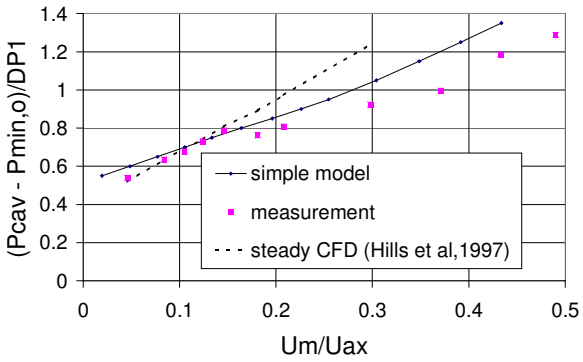

Fig. 14.Comparison of measured and calculated cavity pressure.

Calculated and measured values for the cavity pressure are compared in fig. 14. Results from the steady CFD model of Hills et al (1997) are also included. The experimental values were obtained by extrapolating measurements from tappings at r/r_0=0.90 and r/r_0=0.95 to r/r_0=1.0. All values are normalised by subtracting the minimum annulus pressure at the lowest sealing flow rate and dividing by the peak-to-peak annulus pressure asymmetry. The simple model can be said to be in fair agreement with the measurements. The steady CFD results diverge from the measurements at higher sealing flows. Hills et al considered that this might be due to the neglect of the effect of the sealing flow on the flow in the guide vanes in their CFD model. The better agreement between the simple model and measurement at high flow rates is consistent with this. Using a potential flow solution at inlet to model the annulus pressure asymmetry due to the vanes, the upstream extent of the CFD domain in the annulus was limited. Thus as the upstream influence of the flow ejected from the seal increased with flow rate this effect would not be captured. Although not shown on the figure, further results from the simple model show that the neglect of inertial terms in eqn (7) have only a weak effect on the cavity pressure. This contrasts with a strong effect on sealing effectiveness shown in fig. 12, and suggests that the relative pressures in the cavity and the annulus cannot, on their own, be used to give reliable estimates of ingestion levels.

4.3 Annulus flow losses

As mentioned in the introduction, the non-axisymmetric nature of shroud leakage flows has been noted by workers concerned with the aerodynamic efficiency of the annulus flow. The 3D nature of the flow is particularly clear from the velocity measurements of Pfau et al (2000) and Demargne and Longley (2000). As is consistent with the above discussion of inertial effects, Demargne and Longley's velocity and concentration measurements also show that, in their configuration, increasing the tangential velocity of the sealing flow tends to reduce ingestion.

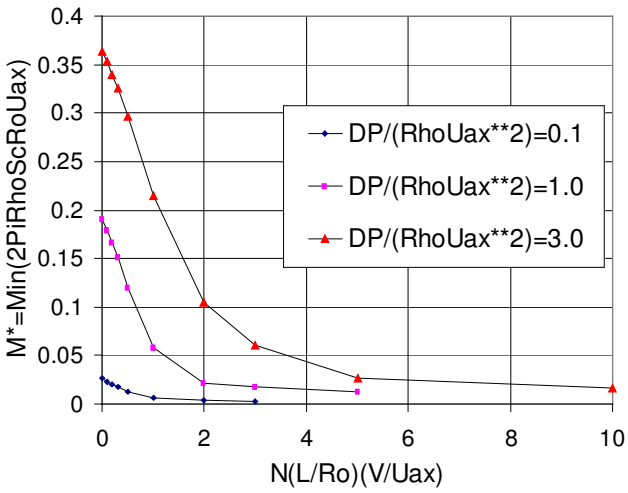

Fig. 15. Calculated mass inflow from simple model for steady conditions with no sealing flow.

While loss generation in the annulus flow due to interaction with the blading flows can be very complex, ingestion and subsequent ejection of mainstream flow through the seal may be important at low sealing flow rates and large sealing gaps. This was noted by Wallis et al (2000). Estimates of the ingestion flow rate when the net sealing flow is zero can be obtained from the simple model. Fig. 15 gives results for the case of a sinusoidal pressure asymmetry for steady flow in which there are no rotor/stator interaction effects. For these conditions the non-dimensional ingestion flow rate ($m^*=m_{in}/2\pi\rho s_c r_o u_{ax}$) is a function of just two parameters; the non-dimensional peak-to-peak pressure asymmetry variation ($\Delta p^*=\Delta p/\rho u_{ax}^2$) and the group $n(l/r_o)(v/u_{ax})$. Direct comparison of these calculations with results from the references mentioned above is difficult. However, very roughly, for Demargne and Longley's case the simple model gives an inflow of about 0.1% of mainstream flow. This is consistent with the measurements. For Wallis et al's case there is little guidance as to the level of pressure asymmetry, but ingress flow rates of around 0.5 to 1% of annulus flow might be estimated for their seal exit cavity. Wallis et al showed that fitting baffles in the seal cavity reduced turbine loss. This was attributed to better alignment of the leakage flow with the annulus flow before it left the cavity. It is possible that the greater tangential velocity of the cavity flow

(relative to the rotating blade) may have contributed to the improvement in loss with some suppression of ingestion.

5. CONCLUSIONS

Mainstream gas ingestion through a model turbine rim seal has been considered using experimental, CFD and more elementary modelling techniques. For the simple model considered reasonable agreement was found between CFD calculations and measurements when both the stator vanes and rotor 'pegs' were included in a full 3D, unsteady CFD simulation. The circumferential pressure asymmetry at the seal generated by the rotor pegs is considerably less than that due to the vanes, but the CFD results show the rotor pegs to have a disproportionately large effect on ingestion. The CFD calculations provide strong support for the view that unsteadiness due to the rotor blade will usually lead to more ingestion. Differences between measured and calculated levels of ingestion may be associated with differences between measured and calculated pressure asymmetries in the annulus. The experiments show some evidence of pressure asymmetry components at lower harmonics than those associated with the blades and vanes. These low harmonics could have slow axial decay rates and may be difficult to avoid both in experimental rigs and in engines.

Swirl velocity is found to be an important parameter in controlling the degree of ingestion. The relatively large effect of the rotor pegs in the CFD simulations is attributed to the swirl velocity in the annulus being close to rotor speed. An element of fluid travelling at the annulus flow swirl velocity will be subject to the radial pressure gradient arising from the rotor pegs which rotate at the same speed. This pressure force will tend to drive the fluid element either into or away from the disc cavity. The same fluid element is subject to a time varying radial force as it moves through the pressure field from the vanes. Since the radial force on the element due to the vanes will vary in direction with time it is less effective in driving flow into the disc cavity.

The simple orifice theory model for gas ingestion has been extended to include some inertial effects due to the swirl velocity. This extended model has had some success in reproducing experimental trends and correlating measurements. In addition to the swirl velocity, the numbers of blades and vanes are shown by the simple model to have a strong influence on ingestion. Considering experiments performed by Demargne and Longley (2000) and Wallis et al (2000) it appears that the flow phenomena identified may also be significant in determining aerodynamic losses in the annulus flow.

While the present results provide encouragement for the application of CFD to turbomachinery rim sealing, there are also areas where further work would be useful. Convergence of the unsteady CFD solution to periodic behaviour is slow due to different flow characteristics for the main annulus and disc cavity. This presently limits application of CFD to this problem, but improvements due to computing advances and improved numerical solution techniques are expected in the future. There is also a need for further work on turbulence models to identify or develop suitable models for both disc cavity and blading aerodynamic flows. Various models are established for use in either disc cavities or blading flows, but no model is yet established for use in both these areas. Further research into these areas and evaluation against experimental data are planned by the present authors.

ACKNOWLEDGMENTS

Much of this work has been funded by Rolls-Royce plc. This is gratefully acknowledged by the authors who would also like to thank their colleague T. Green and P. Smout of Rolls-Royce plc for their help and interest.

REFERENCES

Abe, T., Kikuchi, J. and Takeuchi, H., 1979. An investigation of turbine disc cooling. Paper GT30, 3rd CIMAC Congress, Vienna.

Bayley, F.J. and Owen, J.M., 1970. The fluid dynamics of a shrouded disk system with a radial outflow of coolant. ASME J. Engng Power, vol. 92, pp. 335-341.

Bohn, D., Rudzinski, B., Sturken, N. And Gartner, W., 2000. Experimental and numerical investigation of the influence of rotor blades on hot gas ingestion into the upstream cavity of an axial turbine stage. ASME paper 2000-GT-284.

Campbell, D. A., 1978. Gas turbine disc sealing system design. Proc. AGARD conf. On Seal technology in Gas Turbine Engines, AGARD-CP-237.

Cargill, A.M., 1991. On non-axisymmetric and unsteady effects on rim sealing. Rolls-Royce report.

Chew, J.W., 1989. A theoretical study of ingress for shrouded rotating disc systems with radial outflow. ASME paper 89-GT-187 (also ASME J. Turbomachinery, 113, 91-97).

Chew, J.W., Green, T., and Turner, A.B., 1994. Rim sealing of rotor-stator wheelspaces in the presence of external flow. ASME paper 94-GT-126.

Chew, J.W., Dadkhah, S., and Turner, A.B., 1991. Rim sealing of rotor-stator wheelspaces in the absence of external flow. ASME paper 91-GT-33. (Also ASME J. Turbomachinery, 114, 433-438).

Dadkhah, S., Turner, A.B., and Chew, J.W., 1991. Performance of radial clearance rim seals in upstream and downstream wheelspaces. ASME paper 91-GT-32. (Also ASME J. Turbomachinery, 114, 439-445).

Denton, J. D., 1993. Loss mechanisms in turbomachines, ASME paper 93-GT-435.

Demargne, A.A.J. and Longley, J.P., 2000. The aerodynamic interaction of stator shroud leakage and mainstream flows in compressors. ASME paper 2000-GT-570.

Green, T. and Turner, A.B., 1992. Ingestion into the upstream wheelspaces of an axial turbine stage. ASME paper 92-GT-303.

FLUENT5, 1998. Users guide, Fluent Inc.

Green, T., 1994. Effect of external flow on sealing performance of rotor-stator rim seals. D.Phil. thesis, University of Sussex.

Hamabe, K. And Ishida, K., 1992. Rim seal experiments and analysis of a rotor-stator system with non-axisymmetric main flow. ASME paper 92-GT-160.
Hartsel, J. E., 1972. Prediction of effects of mass-transfer cooling on the blade row efficiency of turbine airfoils. AIAA paper 72-11, 10th Aerospace Sciences Meeting, California, USA.
Hills, N.J., 1996. Development and application of multigrid methods in CFD for turbine rim sealing. D.Phil. thesis, University of Sussex.
Hills, N.J., Chew, J.W., Green, T., and Turner, A.B., 1997. Aerodynamics of turbine rim-seal ingestion. ASME paper 97-GT-268.
Kobayashi, N., Matsumato, M. And Shizuya, M., 1984. An experimental investigation of a gas turbine disc cooling system. ASME J. Engng Gas Turbines and Power, vol. 106, pp. 136-141.
Pfau, A., Treiber, M., Sell. M. And Gyarmarthy, G., 2000. Flow interaction from the exit cavity of an axial turbine blade row labyrinth seal. ASME paper 2000-GT-481.
Phadke, U.P. and Owen, J.M., 1988. Aerodynamic aspects of the rim sealing of gas turbine rotor-stator systems parts 1-3. Int J. Heat and Fluid Flow, vol. 9, pp. 98-117.
Roy, R.P., Xu, G., Feng, J., 2000, Study of main-stream gas ingestion in a rotor-stator disk cavity, AIAA paper, AIAA-2000-3372.
Wallis, A.M., Denton, J.D. and Demargne, A.A.J., 2000, The control of shroud leakage flows to reduce aerodynamic losses in a low aspect ratio, shrouded axial flow turbine. ASME paper 2000-GT-475.
Wellborn, S.R. and Okiishi, T.H., 1998. The influence of shrouded stator cavity flows on multistage compressor performance. ASME paper 98-GT-12.
Virr, G.P., Chew, J.W., and Coupland, J., 1993. Application of computational fluid dynamics to turbine disc cavities. ASME paper 93-GT-89. (Also ASME J. Turbomachinery, 116, 701-708).